HHS Public Access

Author manuscript

Vaccine. Author manuscript; available in PMC 2021 June 02.

Published in final edited form as:

Vaccine. 2020 June 02; 38(27): 4298–4308. doi:10.1016/j.vaccine.2020.04.042.

Dissociation of TRIF bias and adjuvanticity

Katharina Richard[*], **Darren J. Perkins**[*], **Erin M. Harberts**[†], **Yang Song**[‡], **Archana Gopalakrishnan**[*], **Kari Ann Shirey**[*], **Wendy Lai**[*], **Alexandra Vlk**[*], **Anup Mahurkar**[‡], **Shreeram Nallar**[*], **Lynn D. Hawkins**[¶], **Robert K. Ernst**[†], **Stefanie N. Vogel**[*,a]

[*]Department of Microbiology and Immunology, University of Maryland School of Medicine (UMSOM), Baltimore, MD

[†]Department of Microbial Pathogenesis, University of Maryland School of Dentistry (UMSOD), Baltimore, MD

[‡]Genome Informatics Core, Institute for Genome Sciences (IGS), UMSOM, Baltimore, MD

[¶]G2D2, Eisai Inc., Cambridge, MA

Abstract

Toll-like receptors (TLRs), a family of “pattern recognition receptors,” bind microbial and host-derived molecules, leading to intracellular signaling and proinflammatory gene expression. TLR4 is unique in that ligand-mediated activation requires the co-receptor myeloid differentiation 2 (MD2) to initiate two signaling cascades: the MyD88-dependent pathway is initiated at the cell membrane, and elicits rapid MAP kinase and NF-κB activation, while the TIR-domain containing adaptor inducing interferon-β (TRIF)-dependent pathway is initiated from TLR4-containing endosomes and results in IRF3 activation. Previous studies associated inflammation with the MyD88 pathway and adjuvanticity with the TRIF pathway. Gram-negative lipopolysaccharide (LPS) is a potent TLR4 agonist, and structurally related molecules signal through TLR4 to differing extents. Herein, we compared monophosphoryl lipid A (sMPL) and E6020, two synthetic, non-toxic LPS lipid A analogs used as vaccine adjuvants, for their capacities to activate TLR4-mediated innate immune responses and to enhance antibody production. In mouse macrophages, high dose sMPL activates MyD88-dependent signaling equivalently to E6020, while E6020 exhibits significantly more activation of the TRIF pathway (a “TRIF bias”) than sMPL. Eritoran, a TLR4/MD2 antagonist, competitively inhibited sMPL more strongly than E6020. Despite these differences, sMPL and E6020 adjuvants enhanced antibody responses to comparable extents, with balanced immunoglobulin (Ig) isotypes in two immunization models. These data indicate that a TRIF bias is not necessarily predictive of superior adjuvanticity.

Graphical Abstract

[a]Corresponding Author: Stefanie N. Vogel, Ph.D., phone: 410-706-4838, fax: 410-706-8607; svogel@som.umaryland.edu, 685 W. Baltimore St., HSFI-380, Baltimore, MD 21201.

Financial Disclosures

Lynn Hawkins is a scientist with Eisai, Inc. (Cambridge, MA). The other authors have no financial disclosures.

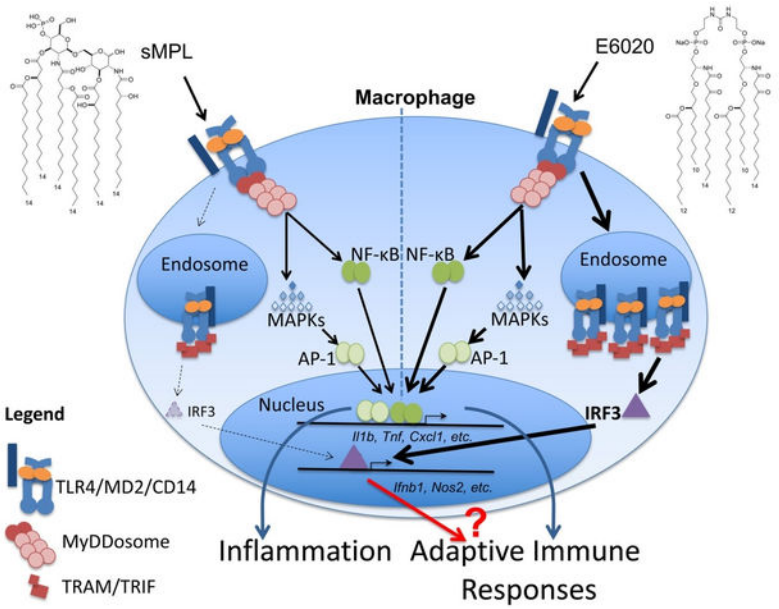

Keywords

Adjuvant; E6020; Lipopolysaccharide; Synthetic monophosphoryl lipid A; Toll-like receptor 4; TRIF bias

Introduction

Vaccine adjuvants rely on their ability to stimulate innate immune responses. One of the most well-studied mechanisms of innate immune activation acts through Toll-Like Receptor 4 (TLR4). The prototype TLR4 agonist is the LPS of Gram-negative bacteria, and, specifically, the lipid A region of LPS, is one of the most potent inflammatory stimuli known [1]. After *in vivo* administration of LPS, proinflammatory cytokines are strongly and rapidly up-regulated and are predominantly macrophage-derived [2]. Macrophage responses contribute to LPS reactogenicity and toxicity. Picogram doses of LPS included in vaccine formulations can improve immunogenicity in mice [3–6]. Immune stimulation by LPS is TLR4-dependent, as evidenced by loss of adjuvanticity in TLR4-deficient mice in various experimental models [7–9]. The non-covalently TLR4-associated proteins CD14 and MD2, are also required to form the higher order signaling complex, TLR4/MD2 [10–12]. The TLR4 antagonist, Eritoran, an inactive lipid A analog, acts by competitively blocking the binding site for the lipid A moiety of LPS on MD2 [10, 13].

Activation of TLR4 signaling at the cell surface leads to recruitment of the adaptor molecule, myeloid differentiation primary response protein 88 (MyD88), triggering formation of a very large, multicomponent structure, the “MyDDosome,” that leads to early activation of the nuclear factor kappa B (NF-κB) and mitogen-activated protein (MAP) kinase signaling pathways [14]. TLR4 may also exhibit CD14-dependent internalization into endosomes [15]. At the endosomal location, the adapters, TRIF-related adaptor molecule (TRAM) and TRIF (a.k.a. TIR-domain containing adaptor molecule 1 (Ticam1)), are

recruited to TLR4 [15], leading predominantly to activation of Interferon Regulatory Factor 3 (IRF3) and production of Type I Interferons (IFN), as well as a delayed wave of NF-κB activation [16]. The Mitchell laboratory first associated activation of the TRIF pathway with adjuvanticity [17], and went on to screen potential synthetic vaccine adjuvants based on their relative ability to elicit TRIF signaling (*i.e.*, a "TRIF bias") [18]. Nonetheless, the molecular mechanism(s) of TRIF-mediated adjuvanticity remains unclear.

Structural analogs of lipid A also signal through TLR4 to varying extents. The best studied of these TLR4-based agonists is bacterially-derived monophosphoryl lipid A (MPL), which is de-toxified by removal of the phosphate group in position 1 [11] and other modifications, but retains strong adjuvanticity [19]. *Salmonella minnesota*-derived MPL is included in several vaccine formulations that are licensed for human use [20]. It later became possible to synthesize MPL structures that retained adjuvant activity [9, 21]. While bacterially-derived MPLs are heterogeneous preparations [22, 23], synthetic MPL (sMPL) produced by Avanti Polar Lipids, LLC (PHAD®), is a homogenous preparation, as evidenced by a single peak in mass spectrometry profiling (m/z 1763, data not shown). Supplementary Figure 1A illustrates the structure of the sMPL used for the present study.

In search of improved synthetic adjuvants, other structural variants of lipid A have been synthesized and tested for toxicity and adjuvanticity [9, 24]. Among these, E6020 (Eisai, Inc.; Supplementary Figure 1B), like sMPL, contains long chain fatty acids that have been shown to interact with TLR4/MD2 [24]. The key difference between sMPL and E6020 is that E6020 is formed with an acyclic flexible linker replacing the phosphorylated sugar backbone of lipid A, which permits dimerization of monovalent phosphate molecules containing three lipids, and greater ease of synthesis [25]. E6020 is also bis-phosphorylated. Compared to LPS, E6020 is also attenuated in its ability to induce fever in rabbits [26], yet in animal models, exhibits potent adjuvant activity [27–37]. The mechanisms underlying differences in adjuvanticity between sMPL and E6020 or related molecules are not known.

To elucidate differences in molecular mechanisms of activation by sMPL and E6020, we conducted experiments that extend prior studies of the potential role of TRIF-dependence in adjuvanticity. Knowledge gained in the intervening years, such as the ability to classify downstream gene expression as being MyD88-dependent, TRIF-dependent, or co-dependent, coupled with more advanced tools to examine TLR4-dependent responses, allowed us to probe TRIF-dependent mechanisms in primary mouse macrophages more critically. Our results demonstrate that E6020 is significantly stronger than sMPL at eliciting TLR4-dependent responses in murine macrophages: while both synthetic TLR4 agonists are highly attenuated compared to LPS, E6020 elicits MyD88-dependent signaling at lower concentrations than sMPL and exhibits significantly greater activation of the TRIF pathway, as evidenced by enhanced TLR4 internalization, IRF3 phosphorylation, and induction of TRIF-dependent genes such as *Ifnb1, Cxcl10,* and *Ccl5*, *i.e.*, a substantial "TRIF bias." Competitive inhibition studies with the TLR4/MD2 antagonist Eritoran [38] revealed that E6020-induced gene expression is less susceptible to inhibition than that induced by sMPL, suggesting that sMPL interacts less strongly with TLR4/MD2. Based on the differential TRIF-biases of E6020 and sMPL, we expected that E6020 would exhibit greater adjuvanticity; however, both sMPL and E6020 elicited equivalent T_H1:T_H2-balanced

antibody responses to both ovalbumin (Ova), a well-established protein antigen, and *Francisella tularensis* LVS nanoparticles, a more complex vaccine [39, 40]. This demonstrates that both strong and weak TRIF-inducing TLR4 agonist adjuvants can stimulate adaptive humoral immune responses comparably. These findings support the conclusion that a "TRIF bias" is not necessarily predictive of improved adjuvanticity.

Materials and Methods

Reagents

LPS was purified from *E. coli* K235 by the hot phenol-water method, as described [41]. Completely synthetic monophosphoryl lipid A (sMPL) was purchased from Avanti Polar Lipids (Cat #699800P; PHAD®) and reconstituted in sterile saline with 0.02% triethylamine (Sigma) and briefly sonicated [42, 43]. Presence of a single sMPL structure was confirmed by mass spectrometry (m/z 1763, data not shown). Synthetic compounds E6020 (TLR4 agonist) and E5564 (TLR4 antagonist; a.k.a. Eritoran), were provided by Eisai, Inc. (Cambridge, MA) and were reconstituted in sterile PBS (E6020; [25]) or endotoxin-free water (E5564; [38]). Sterile fluid thioglycollate was purchased from Remel.

Mice—C57BL/6J mice were purchased from Jackson Laboratories (Bar Harbor, ME 04609). TLR4$^{-/-}$ and Ticam1$^{-/-}$ (TRIF-null) mice were bred at the University of Maryland Baltimore. All experiments involving mice were conducted with institutional approval of the Institutional Animal Care and Use Committee.

Cell culture and stimulation—Unless otherwise indicated, primary mouse thioglycollate-elicited macrophages were harvested by peritoneal lavage in sterile saline [44], and pooled from 2–5 mice per experiment. After a 2 h incubation at 37 ^{o}C, 5% CO_2, peritoneal exudate cells were washed in PBS to remove non-adherent cells. The remaining adherent cells are >98% macrophages [45]. For competitive inhibition assays, cells were pre-treated for 20 minutes with Eritoran (E5564, Eisai Inc.) at concentrations ranging from 0.01 to 100 ng/mL, followed by 2 h stimulation with sMPL or E6020.

Murine RAW 264.7 macrophages (ATCC® TIB-71, passage 6–9) were cultured in RPMI1640 with 10% FBS, 2mM L-glutamine, 100 U/mL Pen/Strep (10% FBS/RPMI complete). Murine MH-S alveolar macrophages (ATCC® CRL-2019) were cultured in 10% FBS/RPMI complete plus 50 μM β-ME medium. Bone marrow derived macrophages (BMDM) were cultured from C57BL/6J bone marrow as previously described [40], using 12.5% LADMAC supernatant as source of M-CSF. Bone marrow derived dendritic cells (BMDC) were cultured from C57BL/6J bone marrow as described by Dr. Ivan Zanoni [46], using 10% B16-GMCSF supernatants (gift from Dr. Zanoni) as source of GM-CSF. Human THP-1 monocytes (ATCC® TIB-202™) were cultured in 10% FBS/RPMI complete plus 10mM HEPES buffer, 1mM sodium pyruvate, and 50 μM β-ME; differentiated into macrophages using 100 nM PMA for 48 h, and "rested" for an additional 24 h before stimulation with TLR4 agonists, as previously described [47].

qRT-PCR—Macrophages were harvested in Tripure reagent (Roche) at the indicated time points after stimulation and frozen at −80 ^{o}C. RNA was extracted by the manufacturer's

protocol and cDNA reverse synthesized from 1 μg RNA per sample using QScript kits (QuantaBio), as previously described [45]. qRT-PCR was performed on a 7900HT instrument (Applied Biosystems) using Power SYBR Green PCR master mix (Applied Biosystems) with primers for *Hprt*, *Tnf, Il10, Il1b, Cxcl1, Ifnb1, Cxcl10*, and *Ccl5* (Sigma, custom synthesis based on published sequences [48], confirmed in primer BLAST). Fold-induction was normalized relative to *Hprt* levels and the medium-treated control levels of individual genes using the $2^{(-\Delta\Delta C_T)}$-method [49].

Western analyses—Immunoblots were performed using antibodies against phosphorylated IRF3 (clone 4D4G), serine 536-phosphorylated NF-κB p65 (clone 93H1), and total IRF3 (clone D93B9) (all from Cell Signaling) as previously described [47].

TLR4 internalization—Macrophages were treated with medium, 100 ng/mL purified LPS, sMPL, or E6020. Samples were collected at 30-minute intervals, chilled to prevent further internalization, Fc-receptors blocked with unconjugated anti-mouse CD16/32 (Clone 93), and stained with Phytoerythrin (PE)-conjugated rat IgG2a anti-mouse TLR4/MD2 (clone SA15–21) or isotype control (clone RTK2758) antibody (BioLegend), and analyzed as previously described [50].

Microarray analysis—Macrophages underwent regular media change (control) or stimulation with 100 ng/mL (57.3 μM) sMPL or 100 ng/mL (61.6 μM) E6020 for 2 h before harvest. Total RNA from 9 samples (3 biological samples/treatment) with RNA integrity number (RIN) values of 8.4 – 10.0, were harvested using High Pure RNA isolation kits (Roche) and hybridized to Affymetrix Clariome D (mouse transcriptome) microarray chips (Thermo Fisher Scientific, Inc.). Differential expression analysis was performed using Affymetrix Transcriptome Analysis Console (TAC) Software Version 4.0. Differentially expressed (DE) genes were identified by threshold of > 2-fold change and a false discovery rate (FDR) < 0.05. Gene expression profiles have been deposited in NCBI's Gene Expression Omnibus [51] database under **GSE131403.** DE gene data were loaded into Ingenuity® Pathway Analysis™ (IPA) for further analysis. Heatmaps and quadrant plots of DE genes were created using ComplexHeatmap, ggplot, and ggrepel packages in R.

Immunizations and antigen-specific ELISAs—Six mice per group were immunized twice, two weeks apart, intramuscularly (i.m.; using a 27G ½" needle) with PBS (negative control), 10 μg EndoFit ovalbumin alone (Ova; Invivogen), Ova + 180 μg Alhydrogel (alum; Invivogen), Ova + 50 μg sMPL, or Ova + 50 μg E6020. Antigen and adjuvants were allowed to adsorb at room temperature for 2 h before injection. Sera were collected weekly and subjected to ELISA on plates coated with 1 μg/well of Ova and developed as previously described [52].

In other experiments, mice were immunized with nanoparticles consisting of catanionic surfactant vesicles containing *Francisella tularensis* (*Ft*) LVS antigens (LVS-V, 35 μg), as described [39], without adjuvant or with 100 μg sMPL or E6020 intraperitoneally (i.p.; using a 25G 5/8" needle), followed two weeks later by intranasal (i.n.; no needle) booster with 5 μg LVS-V, without or with 10 μg sMPL or 3 μg E6020. We previously determined that heterologous (i.p./i.n.) routes of immunization were the most efficacious against i.n.

challenge with virulent *Francisella* [39]. Mice were euthanized, bled, and bronchoalveolar lavage (BAL) performed two weeks post i.n. administration, and antibody titers from sera and BAL fluid (BALf) were determined on *Ft* LVS-coated ELISA plates, as described [40].

Statistics—Statistics for the data in each figure are described in the corresponding figure legend. For microarray data, the FDR (from the Affymetrix TAC output) was used to assess significance. All other statistics and calculations were performed in GraphPad Prism, Version 7. Unless otherwise indicated, graphs show arithmetic mean ± SEM. Comparisons of two experimental groups were performed using the Students *t* test, and comparisons of three or more groups were performed using One-Way ANOVA with Holm-Sidak multiple comparison post-hoc analyses, for which the *p* values were adjusted for the number of comparisons. In Figure 4 (competitive inhibition assays), Eritoran concentration (x) and Fold-Induction (y; calculated as described above) were Log-transformed, and the IC_{50} calculated with Sigmoidal (4-parameter) curve fit. On all graphs, * $p < 0.05$, ** $p < 0.01$, *** $p < 0.001$, and **** or #### $p < 0.0001$.

Results

Analysis of Macrophage gene expression analysis stimulated by TLR4 agonists

Only TLR4 stimulates both the MyD88 and TRIF signaling pathways [1]. To compare the relative TLR4-stimulatory capacities of sMPL and E6020, we initially examined induction of select MyD88-dependent genes (*Il1b, Il10*, and *Tnf*) and TRIF-dependent genes (*Ifnb1, Cxcl10*, and *Ccl5*) by qRT-PCR in dose-response experiments, and included bis-phosphorylated hexa-acylated *E. coli* LPS as a positive control (Figures 1A and 1B). In preliminary experiments, the kinetics of gene induction in response to LPS, sMPL, and E6020 was observed to be comparable (data not shown). Expression of MyD88-dependent genes *Tnf, Il10,* and *Il1b* was induced by both sMPL and E6020 stimulation. Of note, an ~10-fold lower concentration of E6020 was found to elicit gene expression equivalent to that induced by sMPL (Figure 1A). At 100 ng/mL (57.3 μM sMPL, 61.6 μM E6020), however, no significant difference between sMPL and E6020 was observed, reaching similar levels of MyD88-dependent gene expression as the LPS concentration curve plateaued. In contrast, TRIF-dependent genes *Ifnb1, Cxcl10,* and the TRIF and MyD88 co-dependent gene *Ccl5* were only minimally induced by sMPL compared to LPS or E6020, even at the highest concentration tested (Figure 1B). These differential responses were confirmed in RAW 264.7 (mouse macrophages), MH-S (mouse alveolar macrophages), C57BL/6J bone-marrow derived macrophages (BMDM) and dendritic cells (BMDC), as well as in THP-1 (human monocytes, differentiated to macrophages) (Supplementary Figure 2).

To extend our qRT-PCR findings, time-course experiments were performed in which we measured the phosphorylation state of IRF3, the major transcription factor involved in TRIF-dependent TLR4 signaling, and p65, the major species of NF-κB activated in the MyD88-dependent LPS response of macrophages. Figure 1C shows a representative immunoblot using macrophage lysates harvested at 0 to 180 minutes after stimulation with 100 ng/mL of LPS, sMPL, or E6020. E6020 induced a similar degree of IRF3 activation as LPS with increased IRF3 phosphorylation at the 40- and 60-min time points. In contrast, sMPL

induced very little IRF3 phosphorylation, visible only when the immunoblot was overexposed and even at a dose of 1,000 ng/mL, sMPL only weakly induced IRF3 phosphorylation (data not shown). Phosphorylation of NF-κB p65, however, was similar among all treatments. These data support the conclusion that while E6020 and sMPL are both attenuated for MyD88-dependent responses compared to LPS, E6020, but not sMPL, retains the capacity to activate the TLR4-TRIF pathway robustly.

Kinetic differences of TLR4 internalization and signaling in macrophages stimulated with TLR4 agonists

Since TRIF-dependent signaling is dependent upon internalization of the CD14/TLR4/MD2 complex [15, 53], we hypothesized that kinetics of TLR4 internalization in response to sMPL and E6020, would reflect the observed difference in IRF3 activation. Macrophages were stimulated with 100 ng/mL of each TLR4 agonist and internalization rates measured by flow cytometry, a measure of TLR4 translocation to endosomes [15, 50]. Unstimulated cells did not lose surface TLR4 expression over time, while LPS-stimulated cells (positive control) lost surface expression of TLR4 at a rate of 36 ± 2% per hour, as we described [13, 47] ($p < 0.0001$). E6020 induced similar kinetics and degree of TLR4 internalization as LPS, yielding an internalization rate of 33 ± 3% per h ($p < 0.0001$) (Figure 1D). In contrast, stimulation of macrophages with sMPL yielded only 3 ± 3% per h TLR4 internalization ($p < 0.0001$ compared to LPS or E6020 internalization) and was not significantly different from unstimulated macrophages. These data indicate that sMPL stimulation results in lower TRIF-dependent gene expression and IRF3 activation than LPS and E6020 because it poorly induces internalization of the TLR4 receptor complex.

To assess whether enhanced activation of the TRIF-dependent pathway by E6020 truly is TRIF-dependent, stimulation with 100 ng/mL of each TLR4 agonist was carried out in macrophages from C57BL/6J (WT), TLR4$^{-/-}$, and Ticam1$^{-/-}$ (TRIF-null) mice. *Tnf,* our prototypical MyD88-dependent gene, was dependent on the expression of TLR4, but not TRIF, for stimulation with LPS (positive control), sMPL, and E6020. In contrast, the prototypical TRIF-dependent gene *Ifnb1* mRNA expression was diminished in both TRIF- and TLR4-deficient macrophages for all three TLR4 agonists (Figure 1E). Thus, sMPL and E6020 act solely through the TLR4 surface receptor for induction of these genes, and E6020 favors the TRIF-dependent pathway compared to sMPL.

Genome-wide expression analysis of macrophages stimulated by TLR4 agonists

To confirm and extend our findings of differential induction of the TRIF pathway by sMPL and E6020-stimulated macrophages, we performed a microarray analyses of primary mouse peritoneal macrophages that were either untreated (control) or stimulated at 100 ng/mL of the TLR4 adjuvants for 2 h, a dose and time required for optimal induction of many LPS-inducible genes [43]. Total RNA was extracted from three biological replicates (numbered 1–3 for each treatment on the heat map, Figure 2A) and the transcriptomes analyzed by whole transcriptome microarray. Our dataset contained 677 differentially expressed (DE) genes that exhibited a >2-fold difference in any comparison of treatments with a false discovery rate (FDR) < 0.05, of which 94% of DE genes were protein-coding (Supplementary Figure 3A) and were further analyzed. Figure 2A shows the heatmap of

protein-coding genes of each of the biological replicates relative to the average values of each untreated control group. sMPL induced expression of 155 protein-coding (and complex) genes, including those encoding IL-1β, TNF-α, CXCL1, and CXCL2 proteins that are associated with classical macrophage activation and are essential for inducing fever and attracting neutrophils. sMPL treatment of macrophages suppressed only 15 protein-coding genes. In contrast, E6020 induced 413 genes and suppressed 88 genes, including almost all of the sMPL-regulated genes. Lists of DE genes (induced or suppressed >2-fold) by sMPL or E6020 are presented in Supplementary Table I. The quadrant plot compares differential gene expression between the E6020- and the sMPL-stimulated cells (Figure 2B). Symbols between the diagonal lines, spaced at 1 $\log_2$ Fold Change intervals, represent genes that were induced or suppressed to approximately the same extent in sMPL- and E6020-treated cells. Only a single protein-coding gene, platelet derived growth factor B polypeptide (*Pdgfb*), was more highly expressed by sMPL than with E6020 stimulation (2.18-fold). In contrast, 199 protein-coding genes were more highly expressed in E6020-stimulated cells (Table I lists the top 20). The majority of genes induced by E6020, but not sMPL, are associated with Type I IFN expression (Supplementary Figure 3B) [54]. This “interferon signature” supports stronger activation of the TRIF/IRF3 pathway in E6020-treated macrophages and includes genes that are secondarily induced by type I IFNs.

TLR4 signaling can occur either through the MyD88 pathway, initiated at the cell surface, or through the TRIF adaptor from the endosome. Therefore, we selected genes from literature references for their assignments to “MyD88-dependent only,” “TRIF-dependent only,” or “MyD88- and TRIF-dependent” categories (Supplementary Table II) [55–71]. Genes that were strictly dependent on MyD88 for induction, such as *Tnf*, *Cxcl1*, *Cxcl2*, *Ccl3*, and *Il1b*, were induced approximately equally by E6020 and sMPL (E6020/sMPL ratios of 0.86 – 1.84, median 1.22; Figure 2C and Supplementary Table II.A). Genes that were dependent solely on the TRIF adaptor for their induction, such as *Cxcl10*, *Ifit1*, *Mx1*, and *Oasl1*, showed the highest expression in E6020-treated macrophages compared to sMPL-treated macrophages ($p = 0.0062$; Figure 2C, and Supplementary Table II.B). While the majority of TRIF-dependent genes are downstream of IFN-β, we also found differential regulation of TRIF-dependent genes previously reported to be induced independently of Type I IFNs, *e.g., Il6* and *Il33* (Supplementary Table II.B) [56, 65]. Genes regulated by both MyD88- and TRIF-dependent pathways, such as *Ccl2*, *Ccl4, Ccl5, Il1a*, and *Ptgs2*, showed an intermediate pattern of gene induction (Figure 2C, and Supplementary Table II.C). Overall, the microarray analysis shows that E6020 preferentially activates TRIF-dependent genes (*i.e.*, it exhibits a greater “TRIF bias”) than sMPL.

E6020 is less susceptible than sMPL to competitive inhibition of TLR4/MD2

The low rates of TLR4 internalization seen with sMPL prompted us to test the hypothesis that E6020 and sMPL differed in their ability to bind to the TLR4 receptor complex. Eritoran is a TLR4/MD2 antagonist that blocks LPS signaling by competing with LPS for the hydrophobic binding pocket in MD2, thus preventing $(TLR4/MD2)_2$ from reaching the active conformation [10, 13]. Eritoran served as competitive inhibitior in macrophages stimulated with E6020 or sMPL: Macrophages were pretreated with Eritoran for 20 minutes at concentrations ranging from 0.1 to 100 ng/mL. Based on the concentrations of sMPL or

E6020 determined in our prior experiment to induce equivalent *Tnf* mRNA (Figure 1A), we stimulated the cells with either 100 ng/mL sMPL or 10 ng/mL E6020 to achieve similar gene expression levels by 2 h. sMPL was more susceptible to inhibition by Eritoran, with an IC_{50} of 5.6 ng/mL, compared to E6020 with an IC_{50} of 10.9 ng/mL (Figure 3A). Analysis of expression of *Cxcl1* confirmed these findings, with the IC_{50} calculated at 4.1 ng/mL for sMPL and 14.0 ng/mL for E6020 (Figure 3B). Thus, Eritoran inhibited sMPL-induced signaling more readily than E6020-induced signaling. These data suggest that, mechanistically, a reduced interaction of sMPL with the TLR4/MD2 complex likely underlies the reduced receptor internalization and signaling observed.

Stimulation of adaptive humoral immune responses by sMPL vs. E6020

Due to stronger induction of the TRIF-dependent TLR4 signaling pathway and higher resistance to inhibition with Eritoran, we hypothesized that E6020 would also be a more potent vaccine adjuvant than sMPL. Two murine vaccination strategies were employed to test the relative adjuvanticity of E6020 and sMPL. Ova is a well-characterized protein antigen with many tools available to probe immunogenicity, while the *Francisella tularensis* (*Ft*) LVS-functionalized catanionic surfactant vesicle (LVS-V; nanoparticle) antigen presents a more complex antigenic system that is more relevant to vaccine development against bacterial pathogens.

First, mice were immunized i.m. at two-week intervals with PBS, Ova, Ova + alum, Ova + sMPL, or Ova + E6020, and serum collected weekly. The kinetics of Ova-specific IgM, IgG1, and IgG2c titers show that Ova alone elicited weak responses for all three of these major Ig isotypes throughout the course of the experiment. Ova + alum induced high-titer IgG1 starting in week 2, but only minimal levels of IgG2c and IgM. Both sMPL and E6020 adjuvants elicited mildly elevated titers of IgM starting in week 1, as well as high titers of IgG1 and IgG2c starting in week 2, which continued to increase after the boost (Figure 4). Two weeks after the boost, spleen cells were analyzed for lymphocyte subsets by flow cytometry, and no differences were found in the relative proportions of $CD3^+CD4^+$ T cells or $CD3^+CD8^+$ T cells in sMPL- and E6020-adjuvanted groups (data not shown). Even when mice were challenged with Ova antigen after >100 days to elicit memory responses, no difference between sMPL and E6020-induced antibody titers were evident (data not shown).

In a second model of antibody induction, mice were immunized intraperitonally with PBS, empty nanoparticles (V), or *Ft* LVS-functionalized nanoparticles (LVS-V), in the absence or presence of sMPL or E6020. Two weeks later, mice were boosted by i.n. administration, a vaccination regimen found to be the most protective against i.n. challenge with fully virulent *Ft* Schu S4 [39]. Two weeks post-boost, mice were euthanized, and sera and BALf were analyzed for *Ft*-specific antibodies by ELISA. All three immunization groups that included LVS-V (the antigenic nanoparticles) induced comparably high titers of IgG1 (Figure 5A). IgG2c, which is representative of T_H1 immunity [72], was detected in the sera of 12/24 mice immunized with LVS-V alone, and the number of vaccine responders was increased significantly by inclusion of either sMPL (16/18 mice with positive titers) or E6020 (15/16 mice with positive titers) in the vaccine preparations (Figure 5B). In the BALf, both synthetic adjuvants induced approximately 3-fold higher levels of IgG than LVS-V alone

(data not shown), and approximately 15-fold higher levels of IgA than LVS-V alone (Figure 5C). The number of vaccine responders was also increased significantly by either adjuvant for BALf IgA: LVS-V alone only elicited a detectable IgA titer in only 4/16 mice, whereas BALf from 10/13 mice immunized with LVS-V + sMPL, and from 11/16 mice immunized with LVS-V + E6020 showed detectable levels of *Ft*-specific IgA (Figure 5C). These data support the conclusion that sMPL and E6020 are comparable inducers of antibody responses with an improved balance of T_H1:T_H2 responses compared to immunization with antigen alone or antigen plus alum, in both Ova- and LVS-V-immunized mice. Thus, the observed "TRIF bias" elicited by E6020-induced TLR4 signaling did not impart any improvement with respect to adjuvanticity.

Discussion

The need for novel vaccine adjuvants persists, particularly to drive mucosal and cellular T_H1 responses. Early studies showed that LPS itself could be used to enhance adaptive immune responses [3]; however, the toxicity of LPS was prohibitive. *Salmonella*-derived monophosphorylated lipid A (MPL) preparations exhibit low toxicity [19] and are strong, safe adjuvants that are currently included in several licensed human vaccine formulations [20]. However, bacterially derived MPL preparations are heterogenous mixtures of lipid A-like structures, resulting in varying degrees of efficacy, depending on the source. In contrast, synthetic TLR4 agonists show improved structural homogeneity, leading to greater batch-to-batch consistency of responses. Several synthetic TLR4 adjuvants, structurally related to the lipid A region of LPS, have been characterized [9]. sMPL possesses an excellent safety profile (non-reactogenic up to 100 ng/kg in rabbits [33]), but is typically less immunogenic in aqueous formulations [30, 73–75]. The Mitchell laboratory showed that sMPL (phosphorylated only at the 4'-position) is less stimulatory than a similar synthetic LPS-mimetic that was bis-phosphorylated (1 and 4' positions on lipid A) in their study of TRIF-dependent gene expression in bone marrow-derived dendritic cells (DCs) [18]. Nevertheless, several mouse immunization studies show sMPL adjuvanticity *in vivo* [52, 64, 76, 77].

In contrast, E6020 has a bisphosphorylated structure (Supplementary Figure 1), stemming from its synthesis of two monophosphorylated triacyl molecules connected by a flexible acyclic backbone [25]. Yet, E6020 exhibits a very good safety profile, being tolerated up to 30 ng/kg without inducing fever in rabbits, only slightly higher reactogenicity than induced by sMPL, and significantly attenuated compared to LPS (reactogenic at ≤ 0.1 ng/kg) [33].

The mechanism(s) by which lipid A agonists exert their adjuvant effects has been an area of considerable interest for some time. Early work by Henricson *et al.* [43] showed that, at high doses, *Salmonella*-derived MPL induced a number of LPS-inducible genes in macrophages, but at lower concentrations than LPS. Later studies by Mitchell and colleagues correlated the vaccine adjuvanticity of *Salmonella*-derived MPL preparations with the relative ability to induce TRIF-mediated signaling compared to MyD88-mediated signaling [17], leading to the hypothesis that a "TRIF bias" is correlated with adjuvanticity, while MyD88-dependent signaling is associated with inflammation [17, 64, 78–80]. Using bone marrow-derived dendritic cells, this group subsequently showed the sMPL (*i.e.*, the same product as used in our study, but reconstituted with DMSO) was ~10-fold less efficacious in the ability to

induce TRIF-dependent and MyD88/TRIF-co-dependent genes than a synthetic "*E. coli*" lipid A [18]. However, they also reported that synthetic adjuvants induced TRIF-dependent genes at doses that were consistently lower than required for induction of MyD88/TRIF co-dependent gene expression. This established a precedent for the screening of synthetic compounds that could potentially be used as vaccine adjuvants based on their relative ability to elicit TRIF-dependent *vs*. MyD88-dependent signaling.

TRIF-dependent mechanisms have been associated with increased antibody induction: dendritic cell maturation in response to LPS utilizes the TRIF-pathway, as it occurs in MyD88 and mitochondrial antiviral signaling (MAVS) double knockout mice [81], and supplementation of DCs with recombinant Type I IFNs enhances DC maturation [81–83]. Subsequent activation of CD4+ and CD8+ T cells [9], the switch to T_H1-immunity [56], and activation of T-cell independent B cell activation [84], have also been shown to be at least partially TRIF-dependent. Nonetheless, the molecular mechanisms of TRIF-mediated adjuvanticity remain unclear.

Therefore, in an effort to define further the role of TRIF signaling in adjuvanticity, we initially compared sMPL to E6020 for their relative abilities to activate MyD88-dependent *versus* TRIF-dependent genes. Herein, we show that E6020 was a more potent inducer of both pathways. However, at 100 ng/ml, a concentration that elicited nearly equivalent MyD88-dependent gene expression by sMPL and E6020, only E6020 strongly induced TRIF-dependent genes (Figures 1 A–B and 2), findings supported by our observations that sMPL was severely attenuated for stimulating TLR4 internalization that is required for IRF3 activation compared to E6020 and LPS (Figure 1C–D). Together, these data suggest that E6020 is more potent than sMPL for TLR4-dependent macrophage responses. This may be due to a higher affinity for MD2, suggested by the ability of Eritoran, a TLR4 antagonist that acts by binding to MD2, to inhibit sMPL-induced signaling more readily than E6020-induced signaling (Figure 3).

In search of improved TLR4-based vaccine adjuvants, Eisai Inc. developed novel, structurally related lipid A analogs that were easier to synthesize. Ishizaka and colleagues reported that ER-803022 (a precursor to E6020) was a better adjuvant than sMPL [29, 85]. Even though this family of synthetic lipid A mimetics is diphosphorylated [29], E6020 shows low toxicity, similar to sMPL, in contrast to the significantly more inflammatory bis-phosphorylated lipid A [11, 26]. Subsequently, E6020 was advanced as a possible candidate adjuvant and has more recently been used as an adjuvant in small animal models of influenza [28], cytomegalovirus [33], tetanus [29], meningitis [31], chlamydia [34] [33] [34], Chagas disease [27, 32], a *Staphylococcal* enterotoxin B vaccine [30], and an anti-methamphetamine vaccine preparation [37]. E6020 adjuvanticity for mucosal responses was demonstrated at low doses (3 μg/mouse), a dose tolerated by mice when administered by the i.n. route [85]. In most of these published studies, however, E6020 was formulated as an emulsion, which may enhance the adjuvanticity of a vaccine independently of TLR4, as was shown for MPL [74, 75]. To compare the intrinsic adjuvanticity of sMPL and E6020 directly, we used aqueous suspensions of these two synthetic TLR4 agonists. We used IgG2c:IgG1 isotype analysis as surrogate measurement for Th1:Th2 balance, as IgG class switching is highly dependent on Th1 cytokines (*e.g.*, IFN-γ)) for IgG2 and Th2 cytokines

(*e.g.*, IL-4) for IgG1 (reviewed in [72]). As expected from the literature, sMPL and E6020 supported induction of T_H1 immune responses (IgG2c) better than alum (Figure 4). Since E6020 exhibits greater solubility in aqueous solutions than sMPL, it is even more surprising that both adjuvants that differ so significantly with respect to their ability to activate the TRIF pathway, elicited comparable antibody responses *in vivo*, including enhanced titers of IgG1 (T_H2) and IgG2c (T_H1) in the classic Ova-immunization model (Figure 4B–C), as well as significantly reduced rates of non-responders for IgG2c (T_H1) and BALf IgA (mucosal) responses in a complex nanoparticle vaccine model (Figure 5). The enhanced TRIF-signaling in E6020-stimulated animals failed to enhance vaccine responses beyond those induced by sMPL.

To summarize, E6020 is an unusual TLR4 agonist that breaks from the pattern of enhancing adjuvanticity despite significant increases in TRIF-dependent TLR4 signaling. Thus, TRIF-mediated signaling likely has alternate downstream effects apart from mediating increases to adaptive immune responses. Thus, the comparable adjuvanticity of sMPL and E6020 supports the conclusion that “TRIF bias” cannot be used as a proxy for predicting adjuvanticity of novel TLR4 agonists. Further studies are needed to address the divergence in responses downstream of TRIF-activation between E6020 and other TRIF-biased TLR4-agonists that enhance adjuvanticity.

Supplementary Material

Refer to Web version on PubMed Central for supplementary material.

Acknowledgements

This study was supported by grant support from the NIH AI123371 and AI095190 (SNV).

We thank Dr. Ivan Zanoni for providing GM-CSF-rich supernatants and detailed instructions for culturing BMDCs.

Microarray and flow cytometry analyses were performed at the Center for Innovative Biomedical Resources (CIBR) Core Facilities at the University of Maryland, School of Medicine (UMSOM), and we particularly thank Karen Underwood and Jing Yin.

E6020 manuscript abbreviations (alphabetical order)

alum	Alhydrogel
BAL	bronchoalveolar lavage
BALf	bronchoalveolar lavage fluid
CIBR	Center for Innovative Biomedical Resources
DE	differentially expressed
FDR	false discovery rate
Ft	Francisella tularensis
***Ft* LVS**	*Francisella tularensis* Live Vaccine Strain

***Ft* Schu S4**	*Francisella tularensis* Schu S4 Strain (BSL-3)
h	hours
IC_{50}	inhibitory concentration for 50% inhibition
IFN	interferon
Ig	immunoglobulin
i.m.	intramuscular
i.n.	intranasal
i.p.	intraperitoneal
IPA	Ingenuity® Pathway Analysis™
IRF3	interferon regulatory factor 3
LPS	lipopolysaccharide
LVS-V	*Ft* LVS-functionalized nanoparticles (catanionic surfactant vesicles (V))
MAP	mitogen-activated protein
MD2	myeloid differentiation 2
min	minutes
MPL	monophosphoryl lipid A (here, referring to detoxified product of bacterial membranes)
MyD88	myeloid differentiation primary response protein 88
NF-κB	nuclear factor kappa B
Ova	ovalbumin
PE	phytoerythrin
PEC	peritoneal exudate cells
RIN	RNA integrity number
SEM	standard error of the means
sMPL	synthetic monophosphoryl lipid A
T_H1	T helper 1
T_H2	T helper 2
Ticam1	TIR-domain containing adaptor molecule 1 (a.k.a. TRIF)

TLR4	Toll-like receptor 4
TLRs	Toll-like receptors
TRAM	TRIF-related adaptor molecule
TRIF	TIR-domain containing adaptor inducing interferon-β (a.k.a. Ticam1)
V	empty catanionic vesicles (nanoparticles)

References

[1]. Takeda K, Akira S. TLR signaling pathways. Seminars in Immunology. 2004;16:3–9. [PubMed: 14751757]

[2]. Dobrovolskaia MA, Vogel SN. Toll receptors, CD14, and macrophage activation and deactivation by LPS. Microbes and Infection. 2002;4:903–14. [PubMed: 12106783]

[3]. Johnson AG, Gaines S, Landy M. Studies on the O antigen of Salmonella typhosa. V. Enhancement of antibody response to protein antigens by the purified lipopolysaccharide. J Exp Med. 1956;103:225–46. [PubMed: 13286429]

[4]. Lu M, Munford R. LPS stimulates IgM production in vivo without help from non-B cells. Innate Immun. 2016;22:307–15. [PubMed: 27189424]

[5]. Friedman H, Newton C, Blanchard DK, Klein TW, Widen R, Wong KH. Immunogenicity and adjuvanticity of lipopolysaccharide from Legionella pneumophila. Proc Soc Exp Biol Med. 1987;184:191–6. [PubMed: 3809173]

[6]. McAleer JP, Zammit DJ, Lefrancois L, Rossi RJ, Vella AT. The lipopolysaccharide adjuvant effect on T cells relies on nonoverlapping contributions from the MyD88 pathway and CD11c+ cells. J Immunol. 2007;179:6524–35. [PubMed: 17982041]

[7]. Johnson AG. Microbial Adjuvants and Immune Responsiveness In: Friedman H, Klein TW, Szentivanyi A, editors. Immunomodulation by Bacteria and Their Products. Boston, MA: Springer US; 1981 p. 1–11.

[8]. Morrison DC, Ryan JL. Bacterial Endotoxins and Host Immune Responses In: Dixon FJ, Kunkel HG, editors. Advances in Immunology: Academic Press; 1980 p. 293–450.

[9]. Bowen WS, Gandhapudi SK, Kolb JP, Mitchell TC. Immunopharmacology of lipid A mimetics. Adv Pharmacol. 2013;66:81–128. [PubMed: 23433456]

[10]. Kim HM, Park BS, Kim JI, Kim SE, Lee J, Oh SC, et al. Crystal structure of the TLR4-MD-2 complex with bound endotoxin antagonist Eritoran. Cell. 2007;130:906–17. [PubMed: 17803912]

[11]. Park BS, Song DH, Kim HM, Choi BS, Lee H, Lee JO. The structural basis of lipopolysaccharide recognition by the TLR4-MD-2 complex. Nature. 2009;458:1191–5. [PubMed: 19252480]

[12]. Latty SL, Sakai J, Hopkins L, Verstak B, Paramo T, Berglund NA, et al. Activation of Toll-like receptors nucleates assembly of the MyDDosome signaling hub. Elife. 2018;7.

[13]. Rajaiah R, Perkins DJ, Ireland DD, Vogel SN. CD14 dependence of TLR4 endocytosis and TRIF signaling displays ligand specificity and is dissociable in endotoxin tolerance. Proc Natl Acad Sci U S A. 2015;112:8391–6. [PubMed: 26106158]

[14]. Balka KR, De Nardo D. Understanding early TLR signaling through the Myddosome. J Leukoc Biol. 2019;105:339–51. [PubMed: 30256449]

[15]. Kagan JC, Su T, Horng T, Chow A, Akira S, Medzhitov R. TRAM couples endocytosis of Toll-like receptor 4 to the induction of interferon-beta. Nat Immunol. 2008;9:361–8. [PubMed: 18297073]

[16]. Marongiu L, Gornati L, Artuso I, Zanoni I, Granucci F. Below the surface: The inner lives of TLR4 and TLR9. J Leukoc Biol. 2019.

[17]. Mata-Haro V, Cekic C, Martin M, Chilton PM, Casella CR, Mitchell TC. The vaccine adjuvant monophosphoryl lipid A as a TRIF-biased agonist of TLR4. Science. 2007;316:1628–32. [PubMed: 17569868]

[18]. Kolb JP, Casella CR, SenGupta S, Chilton PM, Mitchell TC. Type I interferon signaling contributes to the bias that Toll-like receptor 4 exhibits for signaling mediated by the adaptor protein TRIF. Sci Signal. 2014;7:ra108. [PubMed: 25389373]

[19]. Johnson AG, Tomai MA, Solem LE, Beck L, Ribi E. Characterization of nontoxic monophosphoryl lipid A. Rev Infect Dis. 1987;9:S512–6. [PubMed: 3317747]

[20]. Didierlaurent AM, Laupeze B, Di Pasquale A, Hergli N, Collignon C, Garcon N. Adjuvant system AS01: helping to overcome the challenges of modern vaccines. Expert Rev Vaccines. 2017;16:55–63. [PubMed: 27448771]

[21]. Tomai MA, Vasilakos JP. TLR Agonists as Vaccine Adjuvants In: Baschieri S, editor. Innovation in Vaccinology: from design, through to delivery and testing. Dordrecht: Springer Netherlands; 2012 p. 205–28.

[22]. Hagen SR, Thompson JD, Snyder DS, Myers KR. Analysis of a monophosphoryl lipid A immunostimulant preparation from Salmonella minnesota R595 by high-performance liquid chromatography. Journal of Chromatography A. 1997;767:53–61. [PubMed: 9177005]

[23]. Johnson DA, Sowell CG, Johnson CL, Livesay MT, Keegan DS, Rhodes MJ, et al. Synthesis and biological evaluation of a new class of vaccine adjuvants: aminoalkyl glucosaminide 4-phosphates (AGPs). Bioorg Med Chem Lett. 1999;9:2273–8. [PubMed: 10465560]

[24]. Cluff CW, Baldridge JR, Stover AG, Evans JT, Johnson DA, Lacy MJ, et al. Synthetic toll-like receptor 4 agonists stimulate innate resistance to infectious challenge. Infect Immun. 2005;73:3044–52. [PubMed: 15845512]

[25]. Ishizaka ST, Hawkins LD. E6020: a synthetic Toll-like receptor 4 agonist as a vaccine adjuvant. Expert Rev Vaccines. 2007;6:773–84. [PubMed: 17931157]

[26]. Cekic C, Casella CR, Eaves CA, Matsuzawa A, Ichijo H, Mitchell TC. Selective activation of the p38 MAPK pathway by synthetic monophosphoryl lipid A. J Biol Chem. 2009;284:31982–91. [PubMed: 19759006]

[27]. Seid CA, Jones KM, Pollet J, Keegan B, Hudspeth E, Hammond M, et al. Cysteine mutagenesis improves the production without abrogating antigenicity of a recombinant protein vaccine candidate for human chagas disease. Hum Vaccin Immunother. 2017;13:621–33. [PubMed: 27737611]

[28]. Baudner BC, Ronconi V, Casini D, Tortoli M, Kazzaz J, Singh M, et al. MF59 emulsion is an effective delivery system for a synthetic TLR4 agonist (E6020). Pharm Res. 2009;26:1477–85. [PubMed: 19255727]

[29]. Hawkins LD, Ishizaka ST, McGuiness P, Zhang H, Gavin W, de Costa B, et al. A Novel Class of Endotoxin Receptor Agonists with Simplified Structure, Toll-Like Receptor 4-Dependent Immunostimulatory Action, and Adjuvant Activity. J Pharm Exp Ther. 2002;300:655–61.

[30]. Morefield GL, Hawkins LD, Ishizaka ST, Kissner TL, Ulrich RG. Synthetic Toll-like receptor 4 agonist enhances vaccine efficacy in an experimental model of toxic shock syndrome. Clin Vaccine Immunol. 2007;14:1499–504. [PubMed: 17715328]

[31]. Singh M, Kazzaz J, Ugozzoli M, Baudner B, Pizza M, Giuliani M, et al. MF59 oil-in-water emulsion in combination with a synthetic TLR4 agonist (E6020) is a potent adjuvant for a combination Meningococcus vaccine. Hum Vaccin Immunother. 2012;8:486–90. [PubMed: 22832252]

[32]. Dumonteil E, Bottazzi ME, Zhan B, Heffernan MJ, Jones K, Valenzuela JG, et al. Accelerating the development of a therapeutic vaccine for human Chagas disease: rationale and prospects. Expert Rev Vaccines. 2012;11:1043–55. [PubMed: 23151163]

[33]. Haensler J, Probeck P, Su J, Piras F, Dalencon F, Cotte JF, et al. Design and preclinical characterization of a novel vaccine adjuvant formulation consisting of a synthetic TLR4 agonist in a thermoreversible squalene emulsion. Int J Pharm. 2015;486:99–111. [PubMed: 25794609]

[34]. Visan L, Sanchez V, Kania M, de Montfort A, de la Maza LM, Ausar SF. Phosphate substitution in an AlOOH - TLR4 adjuvant system (SPA08) modulates the immunogenicity of Serovar E

MOMP from Chlamydia trachomatis. Hum Vaccin Immunother. 2016;12:2341–50. [PubMed: 27104338]

[35]. Jones K, Versteeg L, Damania A, Keegan B, Kendricks A, Pollet J, et al. Vaccine-Linked Chemotherapy Improves Benznidazole Efficacy for Acute Chagas Disease. Infect Immun. 2018;86:e00876–17. [PubMed: 29311242]

[36]. Church JS, Milich LM, Lerch JK, Popovich PG, McTigue DM. E6020, a synthetic TLR4 agonist, accelerates myelin debris clearance, Schwann cell infiltration, and remyelination in the rat spinal cord. Glia. 2017;65:883–99. [PubMed: 28251686]

[37]. Arora R, Haile CN, Kosten TA, Wu Y, Ramakrishnan M, Hawkins LD, et al. Preclinical efficacy of an anti-methamphetamine vaccine using E6020 adjuvant. Am J Addict. 2019;28:119–26. [PubMed: 30701618]

[38]. Lynn M, Rossignol DP, Wheeler JL, Kao RJ, Perdomo CA, Noveck R, et al. Blocking of Responses to Endotoxin by E5564 in Healthy Volunteers with Experimental Endotoxemia. The Journal of Infectious Diseases. 2003;187:631–9. [PubMed: 12599080]

[39]. Richard K, Mann BJ, Stocker L, Barry EM, Qin A, Cole LE, et al. Novel catanionic surfactant vesicle vaccines protect against Francisella tularensis LVS and confer significant partial protection against F. tularensis Schu S4 strain. Clin Vaccine Immunol. 2014;21:212–26. [PubMed: 24351755]

[40]. Richard K, Mann BJ, Qin A, Barry EM, Ernst RK, Vogel SN. Monophosphoryl Lipid A Enhances Efficacy of a Francisella tularensis LVS-Catanionic Nanoparticle Subunit Vaccine against F. tularensis Schu S4 Challenge by Augmenting both Humoral and Cellular Immunity. Clin Vaccine Immunol. 2017;24.

[41]. McIntire FC, Sievert HW, Barlow GH, Finley RA, Lee AY. Chemical, physical, biological properties of a lipopolysaccharide from Escherichia coli K-235. Biochemistry. 1967;6:2363–72. [PubMed: 4867999]

[42]. Qureshi N, Takayama K, Ribi E. Purification and structural determination of nontoxic lipid A obtained from the lipopolysaccharide of *Salmonella typhimurium*. J Biol Chem. 1982;257:11808–15. [PubMed: 6749846]

[43]. Henricson BE, Manthey CL, Perera PY, Hamilton TA, Vogel SN. Dissociation of Lipopolysaccharide (LPS)-Inducible Gene Expression in Murine Macrophages Pretreated with Smooth LPS versus Monophosphoryl LipidA. Infect Immun. 1993;61:2325–33. [PubMed: 8388859]

[44]. Dobrovolskaia MA, Medvedev AE, Thomas KE, Cuesta N, Toshchakov V, Ren T, et al. Induction of in vitro reprogramming by Toll-like receptor (TLR)2 and TLR4 agonists in murine macrophages: effects of TLR “homotolerance” versus “heterotolerance” on NF-kappa B signaling pathway components. J Immunol. 2003;170:508–19. [PubMed: 12496438]

[45]. Shirey KA, Cole LE, Keegan AD, Vogel SN. Francisella tularensis Live Vaccine Strain Induces Macrophage Alternative Activation as a Survival Mechanism. The Journal of Immunology. 2008;181:4159–67. [PubMed: 18768873]

[46]. Zanoni I, Tan Y, Di Gioia M, Broggi A, Ruan J, Shi J, et al. An endogenous caspase-11 ligand elicits interleukin-1 release from living dendritic cells. Science. 2016;352:1232–6. [PubMed: 27103670]

[47]. Perkins DJ, Richard K, Hansen AM, Lai W, Nallar S, Koller B, et al. Autocrine-paracrine prostaglandin E2 signaling restricts TLR4 internalization and TRIF signaling. Nat Immunol. 2018;19:1309–18. [PubMed: 30397349]

[48]. Cole LE, Elkins KL, Michalek SM, Qureshi N, Eaton LJ, Rallabhandi P, et al. Immunologic consequences of Francisella tularensis live vaccine strain infection: role of the innate immune response in infection and immunity. J Immunol. 2006;176:6888–99. [PubMed: 16709849]

[49]. Livak KJ, Schmittgen TD. Analysis of relative gene expression data using realtime quantitative PCR and the 2(-Delta Delta C(T)) Method. Methods. 2001;25:402–8. [PubMed: 11846609]

[50]. Richard K, Vogel SN, Perkins DJ. Quantitation of TLR4 Internalization in Response to LPS in Thioglycollate Elicited Peritoneal mouse Macrophages by Flow Cytometry. Bio Protoc. 2019;9.

[51]. Georgakopoulos ND, Wells G, Campanella M. The pharmacological regulation of cellular mitophagy. Nat Chem Biol. 2017;13:136–46. [PubMed: 28103219]

[52]. Gregg KA, Harberts E, Gardner FM, Pelletier MR, Cayatte C, Yu L, et al. A lipid A-based TLR4 mimetic effectively adjuvants a Yersinia pestis rF-V1 subunit vaccine in a murine challenge model. Vaccine. 2018;36:4023–31. [PubMed: 29861179]

[53]. Zanoni I, Ostuni R, Marek LR, Barresi S, Barbalat R, Barton GM, et al. CD14 controls the LPS-induced endocytosis of Toll-like receptor 4. Cell. 2011;147:868–80. [PubMed: 22078883]

[54]. Rusinova I, Forster S, Yu S, Kannan A, Masse M, Cumming H, et al. INTERFEROME v2.0: an updated database of annotated interferon-regulated genes. 41 (database issue): D1040–D1046 ed: Nucleic Acids Research; 2013.

[55]. Hirotani T, Yamamoto M, Kumagai Y, Uematsu S, Kawase I, Takeuchi O, et al. Regulation of lipopolysaccharide-inducible genes by MyD88 and Toll/IL-1 domain containing adaptor inducing IFN-beta. Biochem Biophys Res Commun. 2005;328:383–92. [PubMed: 15694359]

[56]. Weighardt H, Jusek G, Mages J, Lang R, Hoebe K, Beutler B, et al. Identification of a TLR4- and TRIF-dependent activation program of dendritic cells. Eur J Immunol. 2004;34:558–64. [PubMed: 14768061]

[57]. Weighardt H, Mages J, Jusek G, Kaiser-Moore S, Lang R, Holzmann B. Organs-pecific role of MyD88 for gene regulation during polymicrobial peritonitis. Infect Immun. 2006;74:3618–32. [PubMed: 16714594]

[58]. Shaik-Dasthagirisaheb YB, Huang N, Weinberg EO, Shen SS, Genco CA, Gibson FC 3rd. Aging and contribution of MyD88 and TRIF to expression of TLR pathway-associated genes following stimulation with Porphyromonas gingivalis. J Periodontal Res. 2015;50:89–102. [PubMed: 24862405]

[59]. Bjorkbacka H, Kunjathoor VV, Moore KJ, Koehn S, Ordija CM, Lee MA, et al. Reduced atherosclerosis in MyD88-null mice links elevated serum cholesterol levels to activation of innate immunity signaling pathways. Nat Med. 2004;10:416–21. [PubMed: 15034566]

[60]. Bjorkbacka H, Fitzgerald KA, Huet F, Li X, Gregory JA, Lee MA, et al. The induction of macrophage gene expression by LPS predominantly utilizes Myd88-independent signaling cascades. Physiol Genomics. 2004;19:319–30. [PubMed: 15367722]

[61]. Matsushita K, Takeuchi O, Standley DM, Kumagai Y, Kawagoe T, Miyake T, et al. Zc3h12a is an RNase essential for controlling immune responses by regulating mRNA decay. Nature. 2009;458:1185–90. [PubMed: 19322177]

[62]. Suzuki M, Pritchard DK, Becker L, Hoofnagle AN, Tanimura N, Bammler TK, et al. High-density lipoprotein suppresses the type I interferon response, a family of potent antiviral immunoregulators, in macrophages challenged with lipopolysaccharide. Circulation. 2010;122:1919–27. [PubMed: 20974999]

[63]. Thomas KE, Galligan CL, Newman RD, Fish EN, Vogel SN. Contribution of interferon-beta to the murine macrophage response to the toll-like receptor 4 agonist, lipopolysaccharide. J Biol Chem. 2006;281:31119–30. [PubMed: 16912041]

[64]. Coler RN, Bertholet S, Moutaftsi M, Guderian JA, Windish HP, Baldwin SL, et al. Development and characterization of synthetic glucopyranosyl lipid adjuvant system as a vaccine adjuvant. Plos One. 2011;6:e16333. [PubMed: 21298114]

[65]. Polumuri SK, Jayakar GG, Shirey KA, Roberts ZJ, Perkins DJ, Pitha PM, et al. Transcriptional regulation of murine IL-33 by TLR and non-TLR agonists. J Immunol. 2012;189:50–60. [PubMed: 22634618]

[66]. Zenke K, Muroi M, Tanamoto KI. AKT1 distinctively suppresses MyD88-depenedent and TRIF-dependent Toll-like receptor signaling in a kinase activity-independent manner. Cell Signal. 2018;43:32–9. [PubMed: 29242168]

[67]. Huai W, Song H, Wang L, Li B, Zhao J, Han L, et al. Phosphatase PTPN4 preferentially inhibits TRIF-dependent TLR4 pathway by dephosphorylating TRAM. J Immunol. 2015;194:4458–65. [PubMed: 25825441]

[68]. Oldenburg R, Mayau V, Prandi J, Arbues A, Astarie-Dequeker C, Guilhot C, et al. Mycobacterial Phenolic Glycolipids Selectively Disable TRIF-Dependent TLR4 Signaling in Macrophages. Front Immunol. 2018;9:2. [PubMed: 29403489]

[69]. Gu GJ, Eom SH, Suh CW, Koh KO, Kim DY, Youn HS. Suppression of TRIF-dependent signaling pathway of toll-like receptors by (E)-1-(2-(2-nitrovinyl)phenyl)pyrrolidine. Eur J Pharmacol. 2013;721:109–15. [PubMed: 24080550]

[70]. Genin P, Algarte M, Roof P, Lin R, Hiscott J. Regulation of RANTES chemokine gene expression requires cooperativity between NF-kappa B and IFN-regulatory factor transcription factors. J Immunol. 2000;164:5352–61. [PubMed: 10799898]

[71]. Shim DW, Shin HJ, Han JW, Shin WY, Sun X, Shim EJ, et al. Anti-inflammatory effect of Streptochlorin via TRIF-dependent signaling pathways in cellular and mouse models. Int J Mol Sci. 2015;16:6902–10. [PubMed: 25822875]

[72]. Chi X, Li Y, Qiu X. V(D)J Recombination, Somatic Hypermutation and Class Switch Recombination of Immunoglobulins: Mechanism and Regulation. Immunology. 2020.

[73]. Fox CB, Baldwin SL, Vedvick TS, Angov E, Reed SG. Effects on immunogenicity by formulations of emulsion-based adjuvants for malaria vaccines. Clin Vaccine Immunol. 2012;19:1633–40. [PubMed: 22896687]

[74]. Fox CB, Moutaftsi M, Vergara J, Desbien AL, Nana GI, Vedvick TS, et al. TLR4 ligand formulation causes distinct effects on antigen-specific cell-mediated and humoral immune responses. Vaccine. 2013;31:5848–55. [PubMed: 24120675]

[75]. O'Hagan DT, Fox CB. New generation adjuvants--from empiricism to rational design. Vaccine. 2015;33 Suppl 2:B14–20. [PubMed: 26022561]

[76]. Baldwin SL, Shaverdian N, Goto Y, Duthie MS, Raman VS, Evers T, et al. Enhanced humoral and Type 1 cellular immune responses with Fluzone adjuvanted with a synthetic TLR4 agonist formulated in an emulsion. Vaccine. 2009;27:5956–63. [PubMed: 19679214]

[77]. Didierlaurent AM, Morel S, Lockman L, Giannini SL, Bisteau M, Carlsen H, et al. AS04, an aluminum salt- and TLR4 agonist-based adjuvant system, induces a transient localized innate immune response leading to enhanced adaptive immunity. J Immunol. 2009;183:6186–97. [PubMed: 19864596]

[78]. McAleer JP, Rossi RJ, Vella AT. Lipopolysaccharide potentiates effector T cell accumulation into nonlymphoid tissues through TRIF. J Immunol. 2009;182:5322–30. [PubMed: 19380779]

[79]. Rhee EG, Kelley RP, Agarwal I, Lynch DM, La Porte A, Simmons NL, et al. TLR4 ligands augment antigen-specific CD8+ T lymphocyte responses elicited by a viral vaccine vector. J Virol. 2010;84:10413–9. [PubMed: 20631129]

[80]. Bowen WS, Minns LA, Johnson DA, Mitchell TC, Hutton MM, Evans JT. Selective TRIF-dependent signaling by a synthetic toll-like receptor 4 agonist. Science Signaling. 2012;5:ra13. [PubMed: 22337809]

[81]. Hu W, Jain A, Gao Y, Dozmorov IM, Mandraju R, Wakeland EK, et al. Differential outcome of TRIF-mediated signaling in TLR4 and TLR3 induced DC maturation. Proc Natl Acad Sci U S A. 2015;112:13994–9. [PubMed: 26508631]

[82]. Hoebe K, Janssen EM, Kim SO, Alexopoulou L, Flavell RA, Han J, et al. Upregulation of costimulatory molecules induced by lipopolysaccharide and double-stranded RNA occurs by Trif-dependent and Trif-independent pathways. Nat Immunol. 2003;4:1223–9. [PubMed: 14625548]

[83]. Longhi MP, Trumpfheller C, Idoyaga J, Caskey M, Matos I, Kluger C, et al. Dendritic cells require a systemic type I interferon response to mature and induce CD4+ Th1 immunity with poly IC as adjuvant. J Exp Med. 2009;206:1589–602. [PubMed: 19564349]

[84]. Pihlgren M, Silva AB, Madani R, Giriens V, Waeckerle-Men Y, Fettelschoss A, et al. TLR4- and TRIF-dependent stimulation of B lymphocytes by peptide liposomes enables T cell-independent isotype switch in mice. Blood. 2013;121:85–94. [PubMed: 23144170]

[85]. Przetak M, Chow J, Cheng H, Rose J, Hawkins LD, Ishizaka ST. Novel synthetic LPS receptor agonists boost systemic and mucosal antibody responses in mice. Vaccine. 2003;21:961–70. [PubMed: 12547609]

Highlights

- Synthetic lipid A analog adjuvants, E6020 and sMPL, signal through TLR4/MD2.
- E6020 preferentially activates the TRIF-dependent TLR4 signaling pathway.
- E6020 interacts more strongly with TLR4/MD2 and is internalized more rapidly.
- Despite TRIF-bias, E6020 and sMPL exhibit comparable adjuvanticity *in vivo*.
- Conclusion: Our study shows that a “TRIF bias” is dissociable from adjuvanticity.

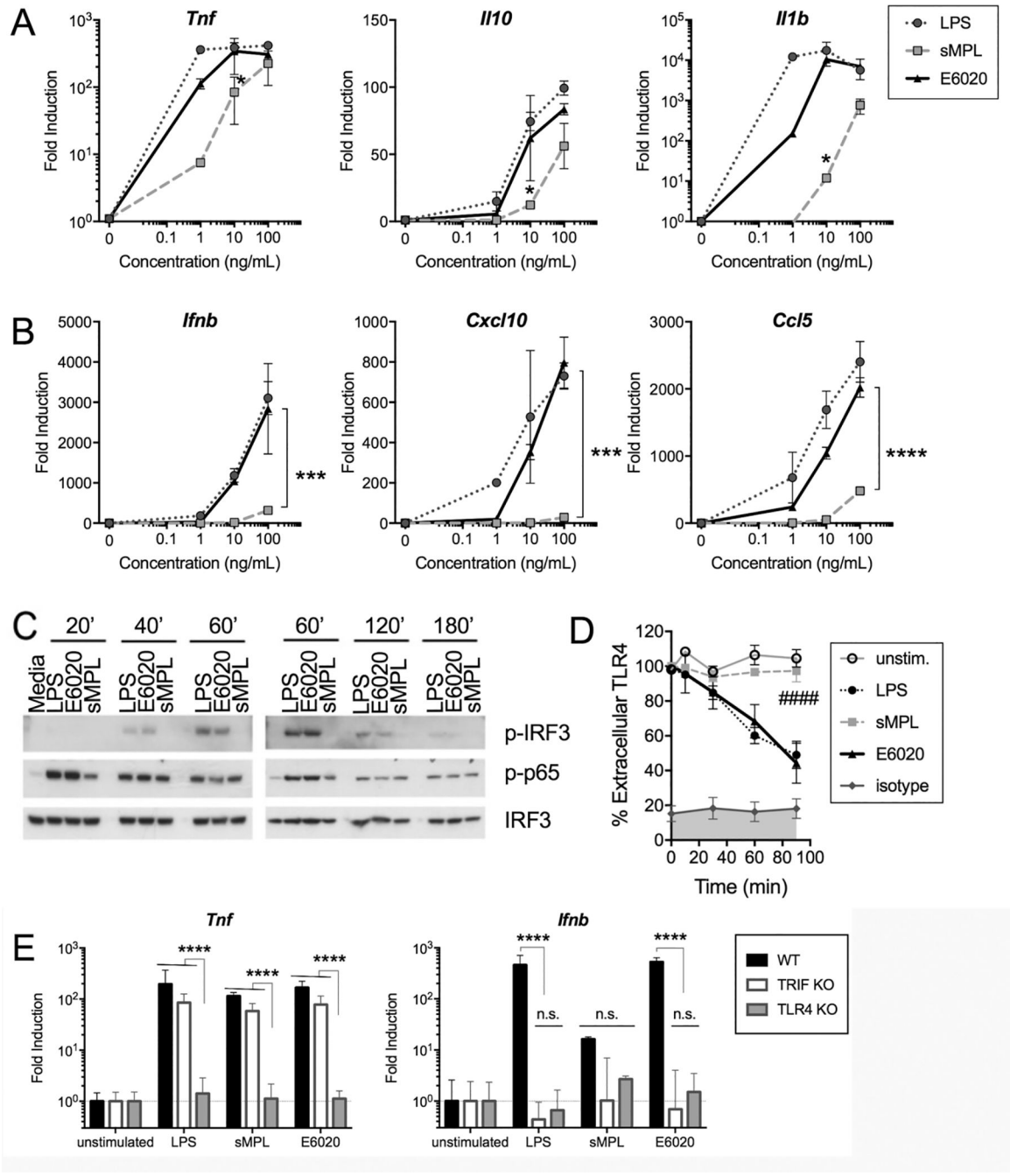

Figure 1. TRIF-dependent genes, IRF3 phosphorylation, and TLR4 internalization are strongly induced in E6020- *vs*. sMPL-stimulated macrophages.

Macrophages were either medium-treated ("0") or treated for the indicated times with 1 – 100 ng/mL of LPS (circle, dotted line), sMPL (square, dashed line), or E6020 (triangle, solid line). qRT-PCR was employed to measure fold-induction over medium-treated baseline gene expression (normalized to *Hprt* mRNA expression) of **(A)** MyD88-dependent genes *Tnf, Il10,* and *Il1b* mRNA, and **(B)** TRIF-dependent genes *Ifnb1* and *Cxcl10*, and MyD88-TRIF co-dependent gene *Ccl5* mRNA. Each graph shows the arithmetic mean ± SEM of a representative experiment of 2–4 separate experiments. Preliminary time-course experiments

for each gene were performed and the maximum gene expression time chosen for dose response curves: *Tnf, Il10,* and *Ifnb1* mRNAs were harvested at 2 h, *Il1b* and *Cxcl10* mRNAs were harvested at 4 h, and *Ccl5* mRNA was harvested at 24 h. Dose response data were analyzed by One-Way ANOVA with post-hoc multiple comparison analyses; E6020 *vs.* sMPL **A:** $p = 0.0167$ (*Tnf*), $p = 0.0005$ (*Il10*), $p = 0.0048$ (*Il1b*), **B:** $p \leq 0.0001$ (*Ifnb1, Cxcl10,* and *Ccl5*). **(C)** Macrophages were treated with 100 ng/mL of the indicated TLR4 agonists and samples collected at the indicated time points (0 – 180 minutes). Western analysis was carried out using anti-phospho-IRF3 antibodies, anti-phospho-p65 antibodies, and anti-total IRF3 antibodies. **(D)** Macrophages were cultured overnight in flow cytometry tubes, and either left untreated or stimulated with 100 ng/mL of LPS, sMPL, or E6020 for 30 – 90 minutes. At each time point, cells were rapidly chilled to prevent further internalization of TLR4, surface-stained with PE-rat IgG2a,κ anti-mouse CD284 (TLR4; clone SA15–21) or isotype control (clone RTK2758), and analyzed by flow cytometry. The percentage of TLR4 remaining on cell surface based on median PE-intensity is shown as arithmetic mean ± SEM of 3 or more independent experiments. TLR4 internalization rates (linear regression model with TLR4/MD2 surface staining levels at 0 min defined as 100%) of the 4 treatment groups were analyzed by One Way ANOVA ($p < 0.0001$) with Holm-Sidak's multiple comparsion post-hoc analysis: ####, LPS or E6020 *vs.* unstimulated cells or sMPL $p < 0.0001$. (**E**) C57BL/6J, TRIF−/−, and TLR4−/− macrophages were stimulated with 100 ng/mL of the respective TLR4 agonists and cytokine expression (*Tnf,* MyD88-dependent; *Ifnb*, TRIF-dependent) measured by qRT-PCR relative to *Hprt.* Differences were assessed by ANOVA with Holm-Sidak posthoc analyses; ****, $p < 0.0001$.

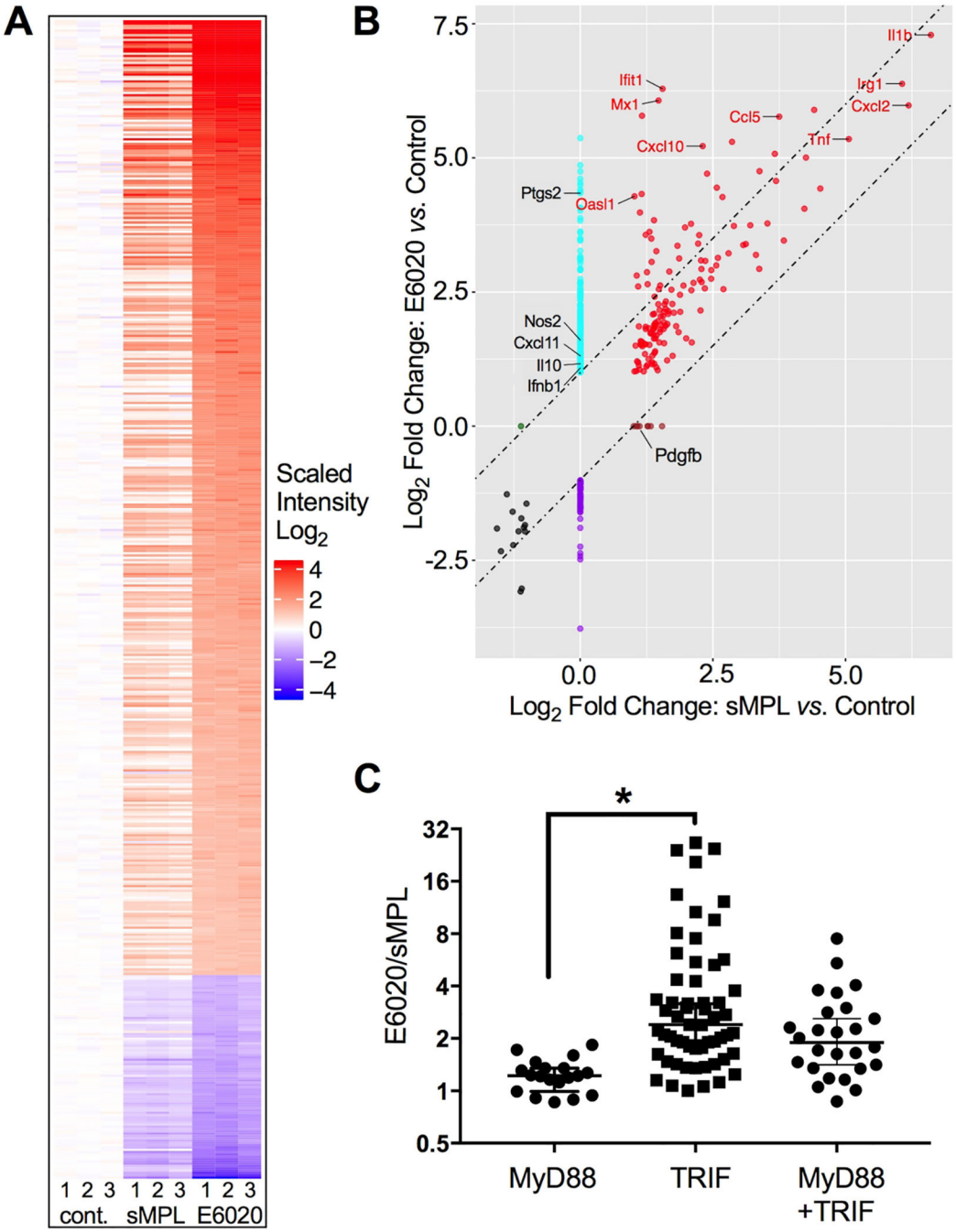

Figure 2. E6020 induces a strong Type I IFN signature.

Primary macrophages were either treated for 2 h with medium only, sMPL, or E6020 (100 ng/mL). RNA was subjected to microarray analysis. **(A)** Heatmap of differentially expressed (2-fold cut-off, FDR < 0.05) protein-coding and complex genes from 3 biological replicates (numbered 1–3 below), that were either left untreated (left), or treated with 100 ng/mL sMPL (middle) or E6020 (right). Each treatment per replicate was assayed on an individual chip. Intensity was plotted relative to the average of the untreated controls. **(B)** Quadrant plot of gene induction/suppression by sMPL *versus* Control (x-axis) and E6020 *versus* Control

(y-axis). Diagonal lines are spaced 1 $\log_2$-fold difference, and genes falling within the lines are equally induced by sMPL and E6020. Genes of particular interest for TLR4-induced, MyD88-dependent and TRIF-dependent activation are labeled. **(C)** The ratio of induction between E6020-treated cells and sMPL-treated cells was calculated for a subset of the differentially expressed genes with previously reported dependence on MyD88, TRIF, or both adapters downstream of TLR4 signaling pathways (Supplementary Table II).

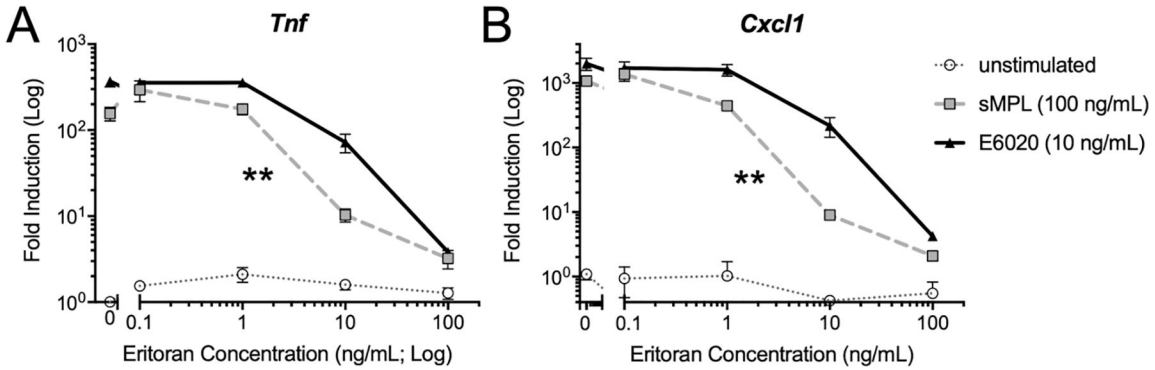

Figure 3. Eritoran is a more potent competitive inhibitor of gene expression induced by sMPL than E6020.

Macrophages were pre-treated with the indicated concentrations of Eritoran, then left untreated (dotted grey line, open circles) or stimulated for 2 h with sMPL (100 ng/mL; dashed grey line, squares) or E6020 (10 ng/mL; solid black line, triangles). These doses were based on equivalent *Tnf* mRNA expression in experiments in Figure 1A. *Tnf* and *Cxcl1* steady-state mRNA levels were measured by qRT-PCR, normalized to mRNA levels for *Hprt* (housekeeping gene). The Eritoran IC_{50} was calculated on the Log-transformed data by Sigmoidal (4PL) curve fit for each TLR4 agonist. A 2-tailed paired Student's *t*-test was used to analyze differences in Eritoran IC_{50} for sMPL *vs.* E6020, $p = 0.0072$ (**). Data were combined from two independent experiments.

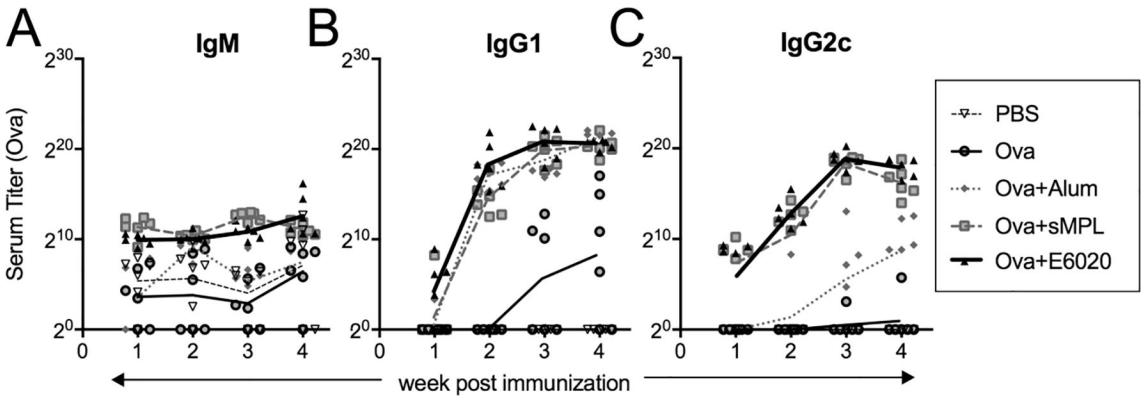

Figure 4. sMPL and E6020 induce comparable antibody titers and Ig isotypes in Ova immunization model.

Mice were immunized i.m./i.m., in weeks 0 and 2, with PBS (open triangle, thin dashed line), Ova (grey circle, thin solid line), Ova + alum (grey diamonds, grey dotted line), Ova + sMPL (grey squares, grey dashed line), or Ova + E6020 (black triangles, thick black line). Sera were harvested weekly and anti-ovalbumin titers of **(A)** IgM, **(B)** IgG1 (T_H2), and **(C)** IgG2c (T_H1) were determined by ELISA. Each symbol represents an individual mouse, and lines connect the geometric means within each treatment group over the time-course. Two-way row-matched ANOVA with Tukey's multiple comparison shows no sustained differences between Ova + sMPL and Ova + E6020 immunizations. IgG1 titers were significantly higher than immunization with Ova alone for groups Ova + Alum ($p < 0.0001$ in weeks 3 and 4) Ova + sMPL ($p = 0.0169$ in week 4) and Ova + E6020 ($p = 0.0214$ in week 4). IgG2c titers were significantly higher than either immunization with Ova alone or Ova + Alum in immunization groups Ova + sMPL (week 3) and Ova + E6020 (weeks 3 and 4), all at $p < 0.0001$.

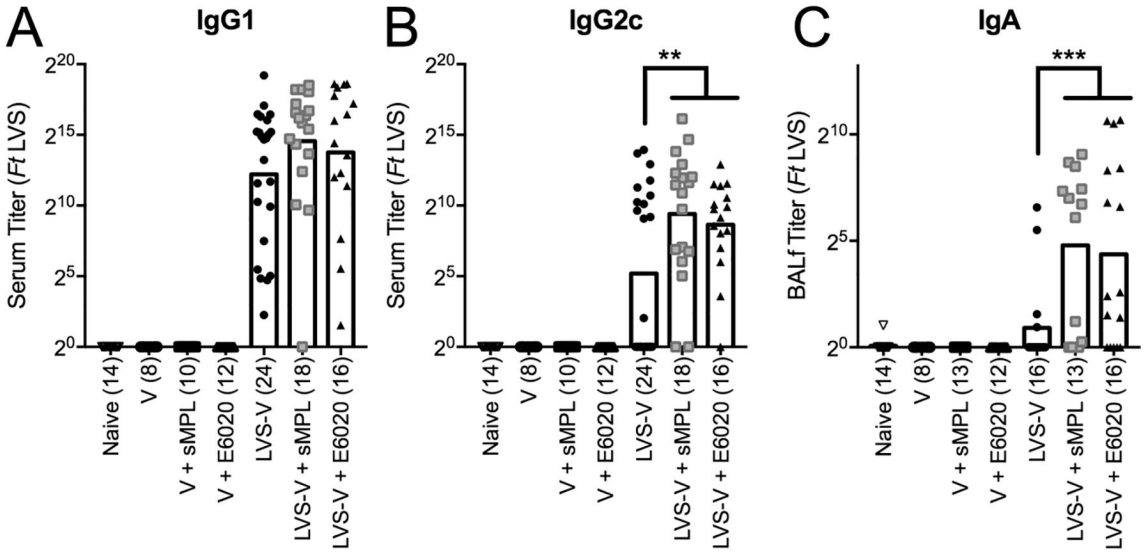

Figure 5. sMPL and E6020 induce similar levels of serum and mucosal antibody responses in the *Ft* LVS-V nanoparticle immunization model.

Mice were immunized i.p./i.n., in weeks 0 and 2, with PBS (open down-triangle), V (open circle), V+sMPL (open square), V+E6020 (open up-triangle), LVS-V (filled circle), LVS-V +sMPL (grey square), or LVS-V+E6020 (filled up-triangle). As all the vaccine 'non-responders' fall on the x-axis, the number of mice in each group (n) is included in parantheses. **(A, B)** Sera and **(C)** BALf were harvested in week 4 and analyzed by ELISA for *Francisella tularensis* (*Ft*)-specific **(A)** IgG1, **(B)** IgG2c, and **(C)** IgA. Each symbol represents the antibody titer from one mouse, and bars show geometric mean of the treatment groups. Data were Log-transformed and analyzed by One-Way ANOVA with Holm-Sidak's multiple comparsions post-tests for LVS-V alone vs. LVS-V+sMPL or LVS-V +E6020, and LVS-V+sMPL *vs.* LVS-V+E6020: **(A)** IgG1: none significant; **(B)** IgG2c: $p = 0.0012$ (LVS-V ± sMPL), $p = 0.0089$ (LVS-V ± E6020); **(C)** BALf IgA: $p = 0.0002$ (LVS-V ± sMPL), $p = 0.0003$ (LVS-V ± E6020).

Table I.

Top 20 protein-coding genes with higher expression in E6020- *versus* sMPL-stimulated macrophages

Fold Change	Gene Symbol	Description
26.64	Ifit1	interferon-induced protein with tetratricopeptide repeats 1
24.66	Mx2	myxovirus (influenza virus) resistance 2
24.17	Mx1	myxovirus (influenza virus) resistance 1
22.91	Tgtp2	T cell specific GTPase 2; T cell specific GTPase 1; T-cell specific GTPase 2
20.07	Trim30c	tripartite motif-containing 30C; novel tripartite motif protein
18.39	I830012O16Rik	RIKEN cDNA I830012O16 gene; novel protein similar to interferon-induced protein with tetratricopeptide repeats 3 Ifit3
15.19	Ifit2	interferon-induced protein with tetratricopeptide repeats 2
15.15	Cmpk2	cytidine monophosphate (UMP-CMP) kinase 2, mitochondrial
14.08	Rsad2	radical S-adenosyl methionine domain containing 2
13.11	Tnfsf4	tumor necrosis factor (ligand) superfamily, member 4
12.22	Usp18	ubiquitin specific peptidase 18
11.95	F830016B08Rik	RIKEN cDNA F830016B08 gene
11.07	Cxcl9	chemokine (C-X-C motif) ligand 9
10.51	Ifit3	interferon-induced protein with tetratricopeptide repeats 3
10.33	Edn1	endothelin 1
9.92	Iigp1	interferon inducible GTPase 1
9.91	Gm4951	predicted gene 4951; novel protein
9.60	Oasl1	2–5 oligoadenylate synthetase-like 1; 2′–5′ oligoadenylate synthetase-like 1
9.02	Tnfsf15	tumor necrosis factor (ligand) superfamily, member 15
8.65	Igtp	interferon gamma induced GTPase